Synergistic role of fission yeast Alp16^{GCP6} and Mzt1^{MOZART1} in γ-tubulin complex recruitment to mitotic spindle pole bodies and spindle assembly

Hirohisa Masuda[a,†,*] and Takashi Toda[a,b]

[a]Lincoln's Inn Fields Laboratory, The Francis Crick Institute, London WC2A 3LY, United Kingdom; [b]Hiroshima Research Center for Healthy Aging, Department of Molecular Biotechnology, Graduate School of Advanced Sciences of Matter, Hiroshima University, Higashi-Hiroshima 739-8530, Japan

ABSTRACT **In fission yeast, γ-tubulin ring complex (γTuRC)–specific components Gfh1^{GCP4}, Mod21^{GCP5}, and Alp16^{GCP6} are nonessential for cell growth. Of these deletion mutants, only *alp16*Δ shows synthetic lethality with temperature-sensitive mutants of Mzt1^{MOZART1}, a component of the γTuRC required for recruitment of the complex to microtubule-organizing centers. γ-Tubulin small complex levels at mitotic spindle pole bodies (SPBs, the centrosome equivalent in fungi) and microtubule levels for preanaphase spindles are significantly reduced in *alp16*Δ cells but not in *gfh1*Δ or *mod21*Δ cells. Furthermore, *alp16*Δ cells often form monopolar spindles and frequently lose a minichromosome when the spindle assembly checkpoint is inactivated. Alp16^{GCP6} promotes Mzt1-dependent γTuRC recruitment to mitotic SPBs and enhances spindle microtubule assembly in a manner dependent on its expression levels. Gfh1^{GCP4} and Mod21^{GCP5} are not required for Alp16^{GCP6}-dependent γTuRC recruitment. Mzt1 has an additional role in the activation of the γTuRC for spindle microtubule assembly. The ratio of Mzt1 to γTuRC levels for preanaphase spindles is higher than at other stages of the cell cycle. Mzt1 overproduction enhances spindle microtubule assembly without affecting γTuRC levels at mitotic SPBs. We propose that Alp16^{GCP6} and Mzt1 act synergistically for efficient bipolar spindle assembly to ensure faithful chromosome segregation.**

Monitoring Editor
Yixian Zheng
Carnegie Institution

Received: Aug 17, 2015
Revised: Mar 23, 2016
Accepted: Mar 29, 2016

INTRODUCTION

Microtubules play essential roles in many cellular processes, such as chromosome segregation, cell division, protein and organelle transport, cell polarity, and cell motility. It is crucial for the cell to spatially and temporally regulate microtubule assembly and its dynamics. γ-Tubulin complexes (γTuCs) are essential for the initiation and regulation of microtubule assembly (reviewed in Kollman *et al.*, 2011; Teixidó-Travesa *et al.*, 2012; Lin *et al.*, 2015; Oakley *et al.*, 2015; Petry and Vale, 2015). γTuCs localize to major microtubule-organizing centers (MTOCs), such as the centrosome in animal cells and the spindle pole body (SPB; the centrosome equivalent) in fungi, as well as to minor MTOCs, such as the nuclear envelope and the Golgi apparatus. In addition, in some systems, the γTuCs localize along the length of microtubules to promote nucleation from the sides of other microtubules.

Two types of γTuCs, the γ-tubulin small complex (γTuSC) and the γ-tubulin ring complex (γTuRC), have been identified in the cell (Kollman *et al.*, 2011; Lin *et al.*, 2015). The γTuSC is composed of γ-tubulin, GCP2, and GCP3. The γTuSC forms a γTuRC ring structure in the presence of GCP4, GCP5, GCP6, and the small protein MOZART1 (Zheng *et al.*, 1995; Moritz *et al.*, 1995, 2000; Murphy *et al.*, 2001; Hutchins *et al.*, 2010). Down-regulation of GCP4, GCP5, or GCP6 disrupts γTuRC assembly (Verollet *et al.*, 2006;

This article was published online ahead of print in MBoC in Press (http://www.molbiolcell.org/cgi/doi/10.1091/mbc.E15-08-0577) on April 6, 2016.

†Present address: Telomere Biology Section, Laboratory of Biochemistry and Molecular Biology, National Cancer Institute, National Institutes of Health, Bethesda, MD 20892.

*Address correspondence to: Hirohisa Masuda (hirohisa.masuda@nih.gov).

Abbreviations used: GFP, green fluorescent protein; γTuC, γ-tubulin complex; γTuRC, γ-tubulin ring complex; γTuSC, γ-tubulin small complex; mCh, monomeric Cherry; mRFP, monomeric red fluorescent protein; MTOC, microtubule-organizing center; SPB, spindle pole body; YES, yeast extract and supplements.

Izumi *et al.*, 2008; Bahtz *et al.*, 2012). The microtubule-nucleating activity of the γTuRC is reminiscent of that of isolated centrosomes (Zheng *et al.*, 1995) and much higher than that of the γTuSC (Oegema *et al.*, 1999).

Two models have been proposed for the roles of γTuRC-specific components in the assembly of the γTuRC ring. In one model, GCP4, GCP5, and GCP6 form a cap-like scaffold that arranges multiple γTuSCs into a ring structure (Moritz *et al.*, 2000; Zhang *et al.*, 2000). In another, more recent model, GCP4, GCP5, and GCP6 are directly incorporated into the ring structure and bind to γ-tubulin (Kollman *et al.*, 2011). The latter is supported by the observed sequence similarity among the GCPs, the structural similarity of GCP4 to GCP2 and GCP3 (Guillet *et al.*, 2011), and the ability of *Drosophila* GCP5 and GCP6 to bind γ-tubulin (Gunawardane *et al.*, 2003). In either case, interaction of the γTuRC-specific components with the MTOCs seems to require their interacting with the γTuSC, since they are not localized to the MTOCs without the γTuSC (Xiong and Oakley, 2009).

In human cells, down-regulation of the γTuRC-specific components GCP4, 5, or 6 reduces γTuC localization at the spindle poles and induces monopolar spindle formation (Izumi *et al.*, 2008; Bahtz *et al.*, 2012). GCP4, 5, and 6, however, are nonessential in the fruit fly *Drosophila melanogaster*, fission yeast *Schizosaccharomyces pombe*, and filamentous fungus *Aspergillus nidulans* (Fujita *et al.*, 2002; Schnorrer *et al.*, 2002; Venkatram *et al.*, 2004; Anders *et al.*, 2006; Verollet *et al.*, 2006; Xiong and Oakley, 2009). The budding yeast *Saccharomyces cerevisiae* does not possess MOZART1 or GCP4, 5, or 6 and only has the γTuSC composed of Tub4/γ-tubulin, Spc97/GCP2, and Spc98/GCP3. Recent studies of the *S. cerevisiae* γTuSC showed that a ring structure could be assembled in vitro from the γTuSC with the help of Spc110, a receptor of the γTuSC at the nuclear side of the SPB (Kollman *et al.*, 2010). Quantification of the number of γTuSC components at microtubule nucleation sites in vivo supports the presence of a spiral of approximately seven γTuSCs at the nucleation site (Erlemann *et al.*, 2012). γTuSC ring assembly may be restricted to SPBs in vivo and temporally regulated by the phosphorylation of the γTuSC and Spc110 (Lin *et al.*, 2014).

These observations imply that two types of ring structure may exist at MTOCs in higher eukaryotes and other fungi—the γTuSC ring assembled on MTOCs from the γTuSCs, and the γTuRC ring recruited from the cytoplasm to the MTOCs. This also raises a question regarding the roles of MOZART1 and GCP4, 5, and 6 in microtubule assembly. In *S. cerevisiae*, the SPBs are the sole MTOCs and nucleate microtubules throughout the cell cycle, whereas most of the MTOCs in higher organisms and other fungi are transiently activated or assembled during the cell cycle. These differences in MTOC activities suggest that MOZART1 and γTuRC-specific components are involved in spatial and temporal regulation of microtubule assembly. In accordance with this, it has been shown that the γTuRC plays a role in microtubule-dependent microtubule nucleation (Verollet *et al.*, 2006) and centriole biogenesis (Bahtz *et al.*, 2012), and that MOZART1 acts as a recruitment factor for the γTuRC to mitotic MTOCs in human cells (Hutchins *et al.*, 2010; Teixidó-Travesa *et al.*, 2010).

In fission yeast, any single deletion of the γTuRC-specific components Gfh1^{GCP4}, Mod21^{GCP5}, and Alp16^{GCP6} and double and triple deletions are viable (Fujita *et al.*, 2002; Venkatram *et al.*, 2004; Anders *et al.*, 2006). Single deletions show a reduction in the cytoplasmic microtubule number and interphase MTOC activity. Double and triple deletions do not lead to additional defects (Anders *et al.*, 2006). No major mitotic defects have been reported in these deletions. In contrast, Mzt1^{MOZART1} is essential for cell growth and is required for the recruitment of γTuCs to all the MTOCs (Masuda *et al.*, 2013; Dhani *et al.*, 2013). We show here the role of Alp16^{GCP6} in mitotic spindle assembly. We find that Alp16^{GCP6} alone functions in mitosis for γTuRC assembly without Gfh1^{GCP4} and Mod21^{GCP5} and that Alp16^{GCP6} and Mzt1 work together for efficient spindle microtubule assembly. We present a model for the synergistic effects of Alp16^{GCP6} and Mzt1 on mitotic γTuRC assembly and activation.

RESULTS

*alp16*Δ is synthetic lethal with a *mzt1* temperature-sensitive mutation

We previously showed that Mzt1 is an essential γTuRC component required for the recruitment of the complex to MTOCs (Masuda *et al.*, 2013). To further study the role of Mzt1 in γTuRC and γTuSC function, we crossed *mzt1-T27W*—a temperature-sensitive *mzt1* mutant strain—with strains in which one of the genes encoding γTuRC-specific components Gfh1^{GCP4}, Mod21^{GCP5}, or Alp16^{GCP6} is deleted. Tetrad dissection showed that *alp16*Δ but not *gfh1*Δ or *mod21*Δ was synthetic lethal with the *mzt1-T27W* mutation (Figure 1A). We examined whether *alp16*Δ shows synthetic lethality with temperature-sensitive mutants of the other γTuSC components and found that *alp16*Δ but not *gfh1*Δ or *mod21*Δ was synthetic lethal with *alp4-1891*, a temperature-sensitive mutant of Alp4^{GCP2} (Vardy and Toda, 2000; Supplemental Figure S1A).

Alp16^{GCP6} is localized to mitotic SPBs without Gfh1^{GCP4} or Mod21^{GCP5} and required for localization of Gfh1^{GCP4} and Mod21^{GCP5} to mitotic SPBs

We studied localization of Gfh1^{GCP4}, Mod21^{GCP5}, and Alp16^{GCP6} at mitotic SPBs using strains expressing the proteins tagged with N-terminal green fluorescent protein (GFP), Sid4–monomeric red fluorescent protein (mRFP), and monomeric Cherry (mCh)–Atb2 (Figure 1B). Sid4-mRFP and mCh-Atb2 were used as SPB and microtubule markers, respectively. GFP-Alp16^{GCP6} localized to the mitotic SPBs in both *gfh1*Δ and *mod21*Δ cells. In contrast, GFP-Gfh1^{GCP4} or GFP-Mod21^{GCP5} did not localize to the mitotic SPBs in *alp16*Δ cells. Gfh1^{GCP4} needed Alp16^{GCP6} but not Mod21^{GCP5} for localization to the mitotic SPBs. Mod21^{GCP5} relied on both Alp16^{GCP6} and Gfh1^{GCP4} for mitotic SPB localization. These results show that the three γTuRC-specific components constitute localization hierarchy: Alp16^{GCP6} acts most upstream, which is followed by Gfh1^{GCP4} and Mod21^{GCP5}. Despite the synthetic lethality with *mzt1* and *alp4* mutants and the disappearance of Gfh1^{GCP4} and Mod21^{GCP5} from mitotic SPBs, *alp16*Δ did not cause an obvious growth reduction (Supplemental Figure S1, D and E).

Levels of γTuC at mitotic SPBs and levels of spindle microtubules are significantly reduced in *alp16*Δ cells

To study the effect of *alp16*Δ on mitotic progression in detail, we observed the dynamic behavior of γTuCs and spindle microtubules in wild-type and *alp16*Δ cells expressing Sid4-mRFP, mCh-Atb2, and GFP-Alp4^{GCP2} or GFP-Mzt1 (Figure 2, A and B). We found that the levels of both Alp4^{GCP2} and Mzt1 at mitotic SPBs and the levels of spindle microtubules were reduced in *alp16*Δ cells compared with wild-type cells. Quantitative analysis showed that GFP-Alp4^{GCP2} and GFP-Mzt1 levels at both mitotic and interphase SPBs in *alp16*Δ cells were reduced to 20–40% of wild-type levels (Figure 2, C and D, and Supplemental Figure S2, C–I). Spindle microtubule levels in *alp16*Δ cells were quantified using GFP-Atb2 to avoid any potential inhibitory effects of GFP tagging of Alp4^{GCP2} and Mzt1 on microtubule nucleation and prevent inaccurate measurement of microtubule levels due to fast photobleaching observed with mCh-Atb2. We found that spindle microtubule levels in *alp16*Δ cells were reduced to

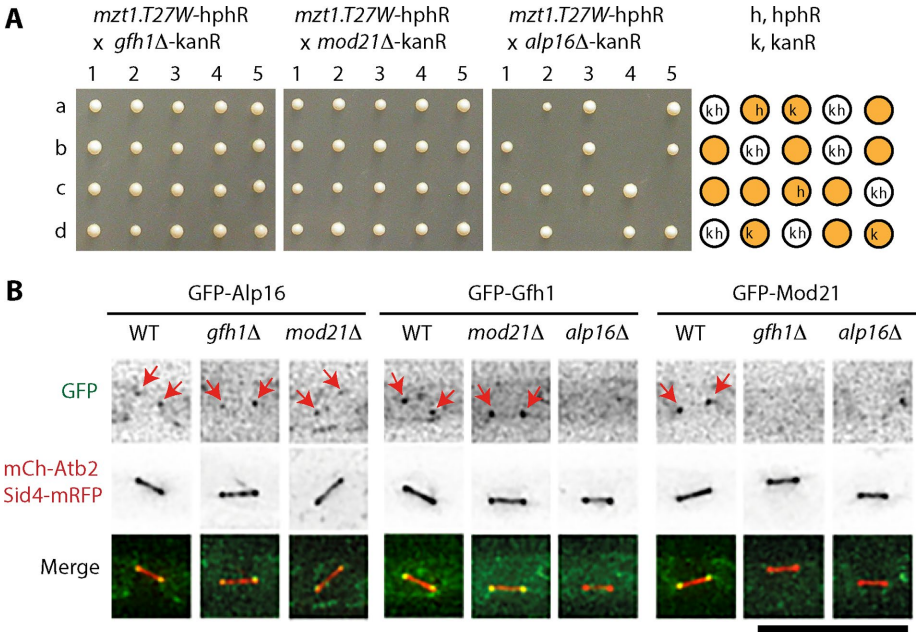

FIGURE 1: *alp16*Δ is synthetic lethal with the *mzt1-T27W* mutant, and Alp16^{GCP6} localizes to mitotic SPBs in the absence of Gfh1^{GCP4} and Mod21^{GCP5}. (A) *alp16*Δ is synthetic lethal with the *mzt1-T27W* mutant. Diploid cells obtained from crosses between *mzt1-T27W-hphR* and *gfh1*Δ*-kanR*, *mod21*Δ*-kanR*, or *alp16*Δ*-kanR* were sporulated, and individual spores (a–d) in each ascus (1–5) were dissected on YES plates. Nonviable spores from the cross between *mzt1-T27W* and *alp16*Δ germinated, divided several times, and arrested with elongated morphologies. Drug resistance of viable spores (orange circle) and predicted resistance of nonviable spores (white circle): k, *kanR* (resistance to G418); h, *hphR* (resistance to hygromycin B). (B) Localization of Alp16^{GCP6}, Gfh1^{GCP4}, and Mod21^{GCP5} to mitotic SPBs. Localization of GFP-Alp16^{GCP6}, GFP-Gfh1^{GCP4}, and GFP-Mod21^{GCP5} to mitotic SPBs was examined in wild-type (WT), *gfh1*Δ, *mod21*Δ, and *alp16*Δ cells containing mCh-Atb2 and Sid4-mRFP. Scale bar, 10 μm.

50–60% of wild-type levels during early M phase and 70–80% during mid M phase (Figure 2E).

Alp16-dependent microtubule assembly is activated in preanaphase spindles

To determine which phase of mitosis is affected by *alp16*Δ, we plotted levels of Alp4^{GCP2}, Mzt1, and spindle microtubules against spindle length (Figure 2, C–E). In wild-type cells, levels of Alp4^{GCP2} and Mzt1 constantly increased, along with increasing spindle length, whereas spindle microtubule levels were high in spindles 1–3 μm long, and levels then decreased when spindles further elongated. Thus, spindle microtubule levels were high in preanaphase spindles, since anaphase spindle elongation was found to begin at a length of ~3 μm on average (Supplemental Figure S3). On the other hand, in *alp16*Δ cells, Alp4^{GCP2} and Mzt1 levels were ~30% of that of wild-type levels upon spindle assembly, which gradually increased as mitosis progressed (Figure 2, C and D). Spindle microtubule levels in *alp16*Δ cells were ~60% of wild-type levels upon spindle assembly, gradually increased until metaphase, and then decreased as the spindle further elongated at anaphase (Figure 2E). The ratio of Alp4^{GCP2} and Mzt1 levels in *alp16*Δ cells to wild- type cells did not change much during mitosis. In contrast, the ratio of spindle microtubule levels in *alp16*Δ cells to wild-type cells was ~60% at prometaphase through metaphase, which then increased to 70% in early anaphase and further increased to 90–100% in late anaphase (Figure 2E). These results suggest that Alp16^{GCP6}-dependent spindle microtubule assembly is prominent during early M phase, especially in preanaphase spindles.

To study whether the deletion of *gfh1* or *mod21*—two genes encoding other γTuRC-specific components—results in the phenotypes similar to *alp16*Δ, we measured the levels of γTuC at the mitotic SPBs and of spindle microtubules from preanaphase spindles (<3.5 μm in length; Figure 2F). Alp4^{GCP2} levels in *gfh1*Δ and *mod21*Δ cells were instead increased to 147 and 111% compared with wild-type cells, whereas Mzt1 levels in *gfh1*Δ and *mod21*Δ cells were decreased to 88 and 72%, respectively. Spindle microtubule levels decreased to 79 and 75% in *gfh1*Δ and *mod21*Δ cells compared with wild-type cells. In contrast, in *alp16*Δ cells, levels of Alp4, Mzt1, and spindle microtubules were reduced to 46, 33, and 39% of wild-type levels, respectively. Thus the *alp16* deletion more specifically and significantly reduced the levels of γTuC at the mitotic SPBs and of spindle microtubules than did the deletion of *gfh1* or *mod21*.

Monopolar spindles are frequently observed before bipolar spindle assembly in *alp16*Δ cells

Our results suggest that the number of microtubules assembled from mitotic SPBs in *alp16*Δ cells is reduced to 60% compared with wild-type cells. To explore the possibility that bipolar spindle assembly is temporarily affected in *alp16*Δ cells, we observed spindle assembly in *alp16*Δ cells expressing GFP-Alp4^{GCP2} and mCh-Atb2 without Sid4-mRFP labeling, which hindered observation of spindle microtubule behavior. About 90% of *alp16*Δ cells showed monopolar spindles or bipolar spindles with extra microtubules emanating from one or both SPBs for 1–3 min, which eventually transformed into stable bipolar spindles (Figure 3, A and B). In contrast, ~60% of wild-type cells showed monopolar or bipolar spindles with extra microtubules for ~1 min, before stable, thick bipolar spindles were assembled (Figure 3B).

In addition to transient monopolar spindle assembly, *alp16*Δ cells remained for longer at the postmitotic stage with equatorial MTOCs, where Alp4^{GCP2} and Mzt1 levels were increased twofold to threefold over wild-type levels (Supplemental Figure S4, A–C). Alp4^{GCP2} and Mzt1 in interphase cells tended to form cytoplasmic dots besides interphase MTOCs, some of which did not seem to be involved in cytoplasmic microtubule formation (Supplemental Figure S4D).

Minichromosome loss rate of *alp16*Δ cells is higher than that of wild-type cells and significantly increased with inactivation of spindle assembly checkpoint

*alp16*Δ cells may show a defect in chromosome segregation if the chromosome number is artificially increased, since reduction in the number of spindle microtubules seems to mostly affect the formation of kinetochore microtubules. To test this possibility, we introduced a minichromosome Ch16 carrying the *ade6-M216* mutation (Niwa *et al.*, 1986) in *alp16*Δ cells that contained the *ade6-M210* mutation. Loss of the minichromosome was detected as red colony or red-sectored colony formation (see *Materials and Methods*). We

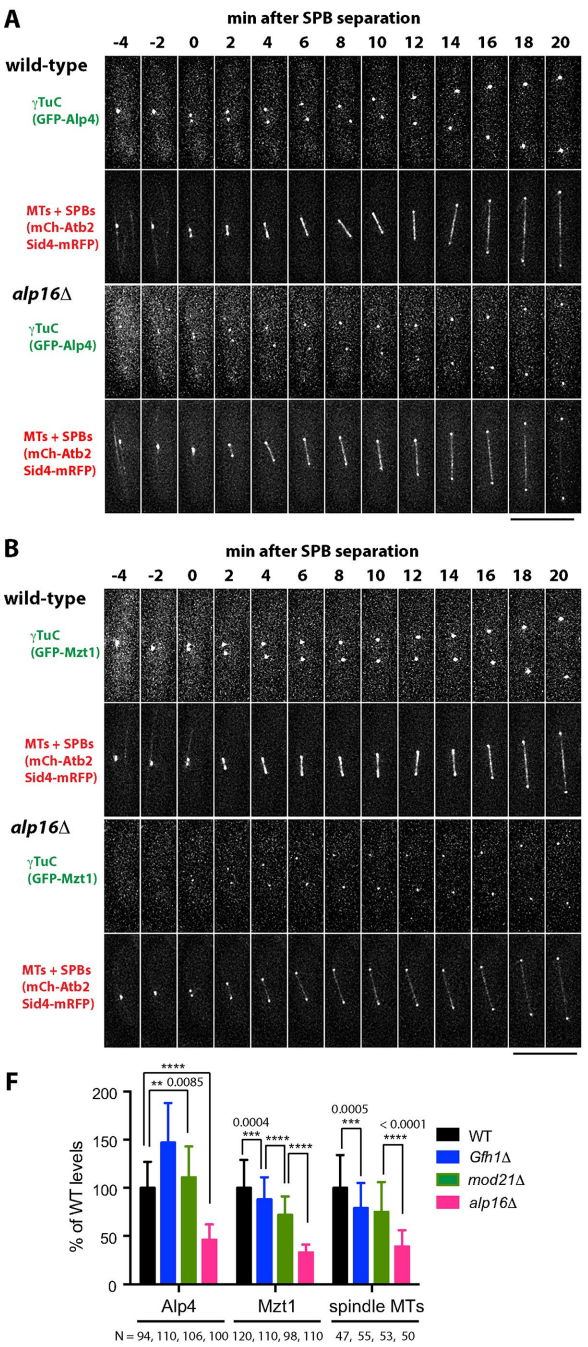

FIGURE 2: *alp16*Δ reduces levels of γTuC at mitotic SPBs and of spindle microtubule levels at early M phase. (A, B) γTuC levels at mitotic SPBs and spindle MT levels are reduced in *alp16*Δ cells. Time-lapse images of wild-type and *alp16*Δ cells containing mCh-Atb2 (for MTs), Sid4-mRFP (for SPBs), and either GFP-Alp4^{GCP2} (A) or GFP-Mzt1 (B) (for γTuC). Time 0 is the time when the two SPBs are separated for spindle assembly. Scale bar, 10 μm. (C, D) Quantification of γTuC levels. Average intensity of GFP signal at mitotic SPBs in wild-type and *alp16*Δ cells expressing GFP-Alp4^{GCP2} (C; $N = 9$ and 8, respectively) or GFP-Mzt1 (D; $N = 12$ and 9, respectively) as a function of time after SPB separation or spindle length. SDs are shown as gray bars. (E) Quantification of spindle microtubule levels. Average intensity of GFP signal for spindles from wild-type ($N = 10$) and *alp16*Δ ($N = 12$) cells expressing GFP-Atb2 as a function of time after SPB separation or spindle length. SDs are shown as gray bars. The *p* values from unpaired *t* test are shown at each time point or spindle length. *$p < 0.05$, **$p < 0.01$, ***$p < 0.001$, and **** $p < 0.0001$. (F) Comparison of γTuC levels at the mitotic SPBs and spindle microtubule levels in wild-type, *gfh1*Δ, *mod21*Δ, and *alp16*Δ cells. γTuC levels at SPBs and spindle microtubule levels from spindles <3.5 μm in length were measured in wild-type, *gfh1*Δ, *mod21*Δ, and *alp16*Δ cells containing GFP-Alp4^{GCP2} or GFP-Mzt1 and mCh-Atb2. The *p* values from unpaired *t* test are shown.

found that *alp16*Δ cells showed a higher loss rate than wild-type cells. Furthermore, *alp16*Δ *mad2*Δ cells showed much higher loss rates, with the spindle assembly checkpoint inactivated by *mad2* deletion (Figure 3C). These results indicate that Alp16^{GCP6}-dependent microtubule nucleation ensures faithful chromosome segregation.

Artificial targeting of Alp16^{GCP6} to Pcp1 at SPBs decreases γTuC levels but increases the ratio of spindle microtubules to γTuC levels

Our results suggest that Alp16^{GCP6} is involved in the recruitment of the γTuRC to mitotic SPBs. Although γTuRC assembly seems to be a prerequisite for localization of γTuRC-specific components to the MTOCs, it is not known whether artificial targeting of the components to the MTOCs affects γTuC levels. We tested whether targeting Alp16^{GCP6} to mitotic SPBs increases γTuRC levels at the SPBs and spindle microtubule levels. Because Pcp1 is likely to act as a receptor for the γTuRC at the mitotic SPB (Fong *et al.*, 2010), we tagged Pcp1 with the GFP-binding protein (GBP; Rothbauer *et al.*, 2008) and used it to target GFP-Alp16^{GCP6} to mitotic SPBs (Figure 4, A and B). GFP-Alp16^{GCP6} levels at mitotic SPBs and spindle microtubule levels were increased in cells expressing both GFP-Alp16^{GCP6} and GBP-Pcp1 (Figure 4, A, C, and E). γTuC levels, represented by mCh-Alp4, at mitotic SPBs, however, decreased in the cells with artificial targeting of Alp16^{GCP6} to Pcp1 (Figure 4, B, D, and E). Thus targeting of Alp16^{GCP6} to Pcp1 had an inhibitory effect on recruitment of the γTuRC or γTuSC to the SPBs. This reduction is probably due to occupation of the γTuC-binding site on Pcp1. Nonetheless, spindle microtubule levels and the ratio of spindle microtubules to γTuC levels at the mitotic SPBs were increased (Figure 4E). These results imply that the γTuRC ring recruited to the SPBs has higher microtubule nucleation activity or assembles more stable microtubules than the nucleating complex assembled from γTuSCs at the SPBs.

Increasing expression levels of Alp16^{GCP6} results in increased levels of γTuC at mitotic SPBs and of spindle microtubules independently of Gfh1^{GCP4} and Mod21^{GCP5}

To further investigate whether the increase in levels of Alp16^{GCP6} at the mitotic SPBs affects γTuC levels and spindle microtubule levels, we changed the expression levels of Alp16^{GCP6}. The *alp16* gene was integrated at the *lys1* locus in *alp16*Δ cells, and expression levels were controlled

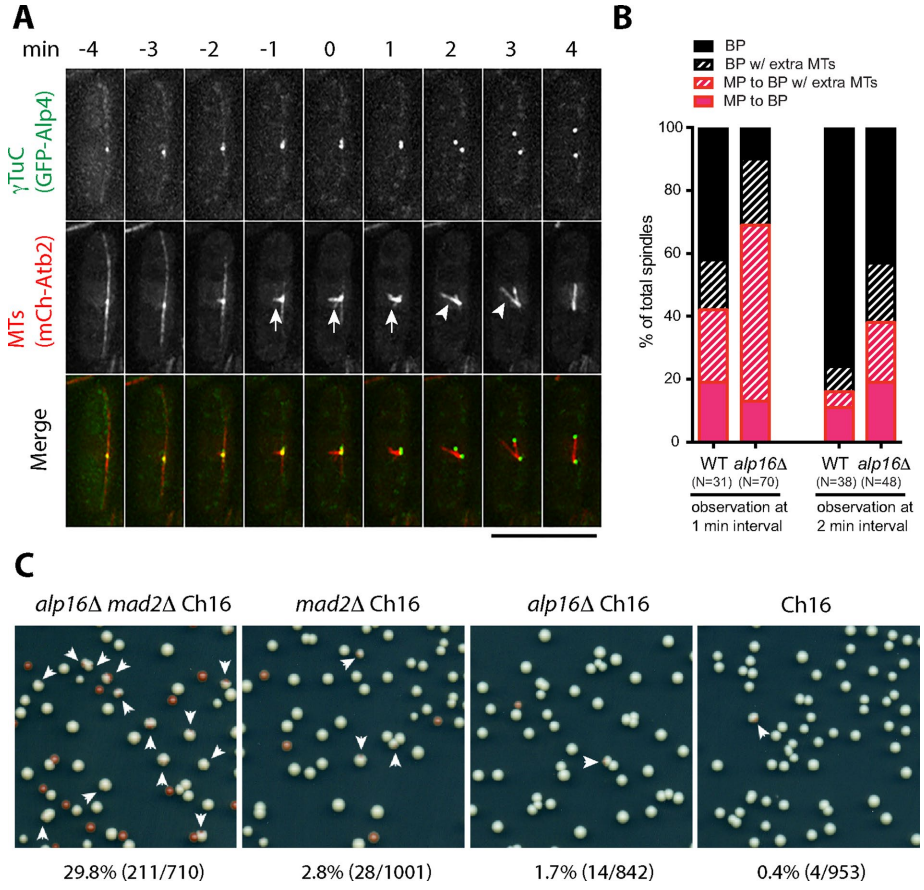

FIGURE 3: *alp16*Δ affects spindle assembly and chromosome segregation. (A) Monopolar spindles observed during early M phase in *alp16*Δ cells. Time-lapse images of an *alp16*Δ cell containing GFP-Alp4^{GCP2} and mCh-Atb2 show formation of a monopolar spindle (arrow), which eventually transforms into a bipolar spindle. A bipolar spindle with an extra microtubule bundle nucleating from the SPB (arrowhead) is observed at 2 and 3 min after SPB separation. Scale bar, 10 μm. (B) Percentages of wild-type and *alp16*Δ mitotic cells with monopolar (MP) spindles or bipolar (BP) spindles with extra microtubule bundles from time-lapse imaging at 1- and 2-min intervals. MP to BP, monopolar spindles transform into bipolar spindles. MP to BP w/extra MTs, monopolar spindles transform into bipolar spindles with extra microtubule bundles, which eventually transform into bipolar spindles. BP w/extra MTs, without monopolar spindle assembly, bipolar spindles with extra microtubule bundles form, which eventually transform into bipolar spindles. BP, bipolar spindles form without monopolar spindle assembly. (C) *alp16*Δ cells frequently lose a minichromosome in the absence of Mad2. *alp16*Δ *mad2*Δ *ade6-M210* Ch16, *mad2*Δ *ade6-M210* Ch16, *alp16*Δ *ade6-M210* Ch16, and *ade6-M210* Ch16 cells were grown at 27°C on YE plates for 6 d. Arrows indicate red-sectored colonies that lost Ch16 during the 6 d of growth. The chromosome loss rate was calculated as the percentage of red-sectored colonies out of the sum of red-sectored and white colonies.

from a thiamine-repressible *nmt1* promoter and its derivatives that have lower activities (Basi *et al.*, 1993). We found that the levels of γTuC at the SPBs and levels of spindle microtubules increased along with the increase in expression levels of Alp16^{GCP6} (Figure 5, A–C).

To study the effect of Alp16^{GCP6} expression on γTuC levels and spindle microtubule levels in more detail, we plotted spindle microtubule levels against γTuC levels (Figure 5D, left). We then plotted ratio of spindle microtubules to γTuC levels at the mitotic SPBs relative to those of *alp16*Δ and wild-type cells against γTuC levels (Figure 5D, right). At a low expression level (under the control of P81*nmt* promoter in the presence of thiamine), γTuC levels at mitotic SPBs were not increased significantly compared with levels in *alp16*Δ cells (by ~11% of wild-type levels). However, spindle microtubule levels significantly increased by ~27% compared with those in *alp16*Δ cells. The ratio of spindle microtubules to γTuC levels increased by ~29% compared with *alp16*Δ cells with similar γTuC levels, suggesting again that the γTuRC ring has a higher activity or forms more stable microtubules compared with the nucleating complex assembled from γTuSCs without Alp16. At medium expression levels (under the control of P41*nmt* and P3*nmt* promoters in the presence of thiamine), spindle microtubule levels reached those of wild-type cells (~97%). with lower levels of γTuC at the SPBs (~77%), or increased to levels higher than wild type (~118%), with levels of γTuC similar to those of wild-type cells (~91%). At high expression levels (with P81 and P41*nmt* promoters in the absence of thiamine), both γTuC levels at SPBs and spindle microtubule levels were higher than those in wild-type cells (Figure 5, B and D). At these medium and high expression levels, the ratio of spindle microtubules to γTuC levels increased compared with wild-type cells.

To study whether Gfh1^{GCP4} and Mod21^{GCP5} are required for the Alp16^{GCP6}-dependent increase in levels of γTuC at mitotic SPBs and of spindle microtubules, we examined localization of GFP-Gfh1^{GCP4} and GFP-Mod21^{GCP5} in cells overproducing Alp16^{GCP6}. Both components were found to localize at the mitotic SPBs (Figure 5E). Next, we overexpressed Alp16^{GCP6} in *alp16*Δ *gfh1*Δ and *alp16*Δ *gfh1*Δ *mod21*Δ cells and found that the Alp16^{GCP6}-dependent increase in levels of γTuC at the mitotic SPBs and of spindle microtubules did not require Gfh1^{GCP4} or Mod21^{GCP5} (Figure 5F).

Alp16^{GCP6} overproduction suppresses the temperature sensitivity of *mzt1* mutant cells but not the lethality of *mzt1*Δ cells

Our results suggest a role for Alp16^{GCP6} in the recruitment of the γTuRC to SPBs. Because Mzt1 is an essential component that acts as a recruitment factor for the γTuRC (Masuda *et al.*, 2013), we examined whether increased levels of Alp16^{GCP6} suppress the phenotype of *mzt1* temperature-sensitive mutants. Serial dilution spot assays showed that overproduction of Alp16^{GCP6} suppressed the temperature sensitivity of *mzt1-T27W* (Figure 6A). Next, to test whether Alp16^{GCP6} overproduction rescues the lethality of the *mzt1* deletion, we constructed diploid cells in which Alp16^{GCP6} was overproduced and one of the *mzt1* genes was deleted. Tetrad analysis showed that Mzt1 was essential for growth even in the cells overproducing Alp16^{GCP6} (Figure 6B). This result suggests that Alp16^{GCP6}, when overproduced, could rescue compromised Mzt1 functions but still is not capable of substituting for its essential roles.

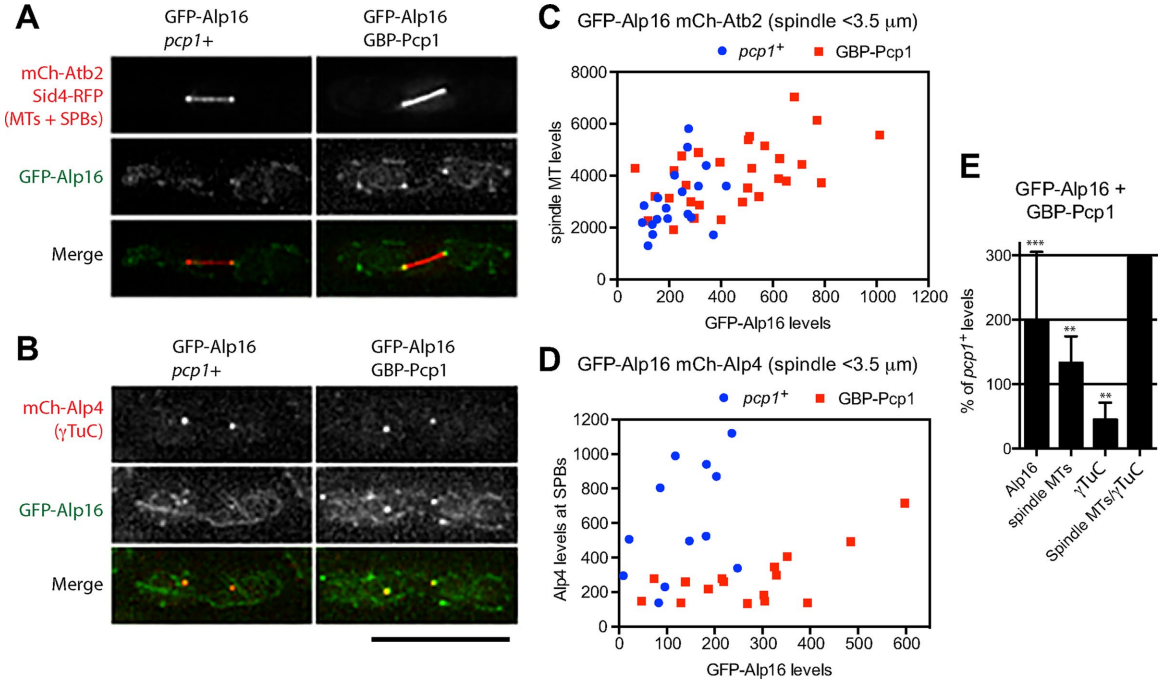

FIGURE 4: Artificial targeting of Alp16^{GCP6} to Pcp1 increases ratio of spindle microtubules to γTuC levels. (A) Targeting of GFP-Alp16^{GCP6} to GBP-Pcp1 in cells expressing mCh-Atb2 increases spindle microtubule levels. Spindles observed in GFP-Alp16^{GCP6} and GFP-Alp16^{GCP6} GBP-Pcp1 cells expressing mCh-Atb2 and Sid4-mRFP. (B) Targeting of GFP-Alp16^{GCP6} to GBP-Pcp1 in cells expressing mCh-Alp4^{GCP2} reduces γTuC levels at mitotic SPBs. Spindles observed in GFP-Alp16^{GCP6} and GFP-Alp16^{GCP6} GBP-Pcp1 cells expressing mCh-Alp4^{GCP2}. Scale bar, 10 μm. (C) Quantification of spindle microtubule levels at mitotic SPBs in cells with or without Alp16^{GCP6} targeting to Pcp1. GFP-Alp16^{GCP6} and mCh-Atb2 levels for spindles <3.5 μm in length were quantified. The sum of GFP-Alp16 levels at two SPBs of mitotic spindles is plotted against mCh-Atb2 levels. (D) Quantification of γTuC levels at mitotic SPBs in cells with or without Alp16^{GCP6} targeting to Pcp1. GFP-Alp16^{GCP6} and mCh-Alp4^{GCP2} levels for spindles <3.5 μm in length were quantified. (E) Levels of Alp16^{GCP6}, spindle microtubules, and γTuC, and the ratio of spindle MTs to γTuC levels in GFP-Alp16^{GCP6} GBP-Pcp1 cells were compared with those in GFP-Alp16^{GCP6} *pcp1*$^+$ cells. The *p* value is from unpaired *t* test: ***$p = 0.0003$ for Alp16^{GCP6} ($N = 19$ for *pcp1*$^+$ and 29 for GBP-Pcp1 cells), **$p = 0.0075$ for spindle microtubules ($N = 19$ for *pcp1*$^+$ and 29 for GBP-Pcp1 cells), and **$p = 0.0017$ for γTuC ($N = 12$ for *pcp1*$^+$ and 16 for GBP-Pcp1 cells).

Mzt1 increases spindle microtubule levels without affecting γTuC levels at mitotic SPBs in wild-type cells

Because augmented Alp16^{GCP6} suppressed the temperature sensitivity of *mzt1* mutants, we examined whether higher levels of Mzt1 in turn suppress the phenotypes of *alp16*Δ cells. Mzt1 overproduction in *alp16*Δ cells had no effect on γTuC levels at mitotic SPBs or spindle microtubule levels (Figure 7A). Unexpectedly, however, overproduction of Mzt1 in wild-type cells increased spindle microtubule levels without affecting γTuC levels at mitotic SPBs (Figure 7A). To determine whether the ratio of Mzt1 to Alp4^{GCP2} is constant or variable during mitotic progression, we calculated the ratio of GFP-Mzt1 to GFP-Alp4^{GCP2} using the average intensity of GFP signal obtained from mitotic GFP-Mzt1 and GFP-Alp4^{GCP2} cells (Figure 2, C and D, and Supplemental Figure S5) and plotted it against spindle length (Figure 7B). The ratio was found to be high in preanaphase spindles 1–3 μm in length compared with that of anaphase spindles in wild-type cells. The ratio did not change substantially in *alp16*Δ cells and stayed low compared with wild-type cells. To confirm the increase in ratio of Mzt1 to Alp4^{GCP2} at early M phase, we directly measured Mzt1 and Alp4^{GCP2} levels in GFP-Alp4^{GCP2} mCh-Mzt1 cells. The ratio of Mzt1 to Alp4^{GCP2} in mitotic cells with preanaphase spindles was found to be higher than that in interphase cells (Figure 7C), suggesting that the number of Mzt1 proteins per γTuRC increases at early M phase.

DISCUSSION

Roles of γTuRC-specific components in spindle microtubule assembly

We showed here that Alp16^{GCP6} but not Gfh1^{GCP4} or Mod21^{GCP5} has demonstrable mitotic function in fission yeast. Levels of γTuC at mitotic SPBs and spindle microtubule levels are significantly reduced in *alp16*Δ cells. This reduction is not observed in *gfh1*Δ or *mod21*Δ cells. We also found that Alp16^{GCP6} expression in *alp16*Δ and *alp16*Δ *gfh1*Δ *mod21*Δ cells results in an increase in these levels (Figure 5). These Alp16^{GCP6}-specific effects are consistent with the interaction hierarchy of the γTuRC-specific components with the γTuSC (Anders *et al.*, 2006) and the hierarchy of localization of components to mitotic SPBs observed in this study: Alp16^{GCP6} alone can interact with the γTuSC and localize to mitotic SPBs without Gfh1^{GCP4} and Mod21^{GCP5}, whereas Gfh1^{GCP4} and Mod21^{GCP5} require Alp16^{GCP6} for interaction with the γTuSC and for localization to mitotic SPBs. Without Alp16^{GCP6}, the number of spindle microtubules nucleated from the SPBs is reduced but is still large enough to form kinetochore microtubules for all three chromosomes in fission yeast without any noticeable mitotic delay. Monopolar spindle assembly is observed more frequently but is eventually converted into a bipolar spindle. Increasing the number of chromosomes from three to four by introduction of a minichromosome reduces the number of microtubules used for kinetochore microtubule formation and dramatically

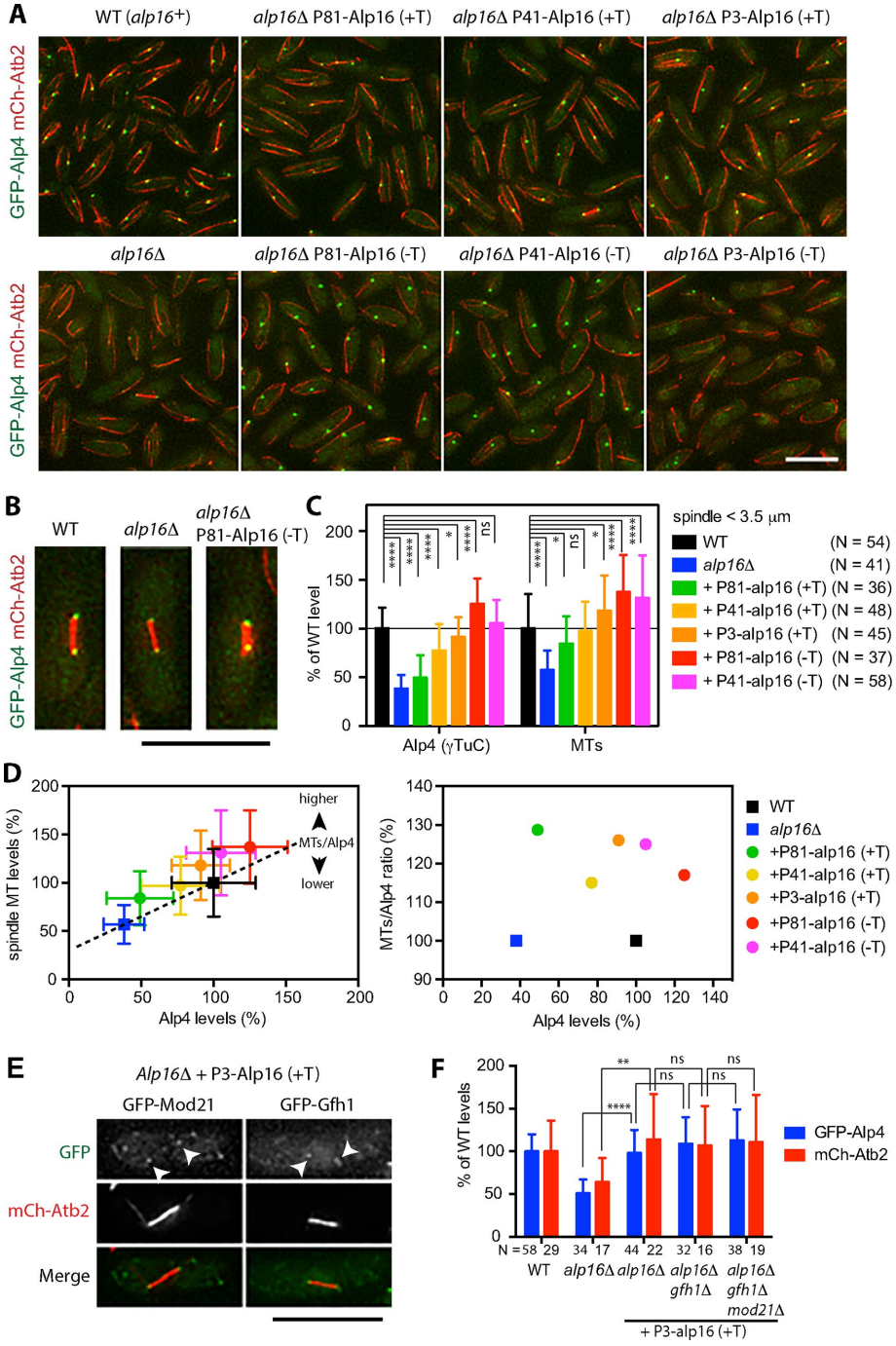

FIGURE 5: Elevated Alp16^{GCP6} expression increases γTuC levels at mitotic SPBs and spindle microtubule levels. (A) Increase in expression levels of Alp16^{GCP6} increases γTuC levels at SPBs. Alp16^{GCP6} was expressed at the *lys1* locus in *alp16*Δ cells containing GFP-Alp4^{GCP2} and mCh-Atb2 under the control of thiamine-repressible P81*nmt*, P41*nmt*, or P3*nmt* promoter in the presence (+T) and absence (–T) of 2 μM thiamine at 27°C for 22–24 h. Alp16^{GCP6} expression levels were the lowest under the P81*nmt* promoter with thiamine (P81-Alp16 (+T)) and increased in the following order: P81 (+T) < P41 (+T) < P3 (+T) < P81 (–T) < P41 (–T) < P3 (–T). The intensity of GFP-Alp4^{GCP2} signals at SPBs increases along with the increase in expression levels of Alp16^{GCP6} but decreases at the highest expression with P3*nmt* promoter in the absence of thiamine. Scale bar, 10 μm. (B) Typical images of spindles observed in wild-type, *alp16*Δ, and *alp16*Δ cells with P81*nmt*-Alp16 (–T). Note that spindles look thicker with higher levels of γTuC at SPBs. (C) Elevated Alp16^{GCP6} expression increases γTuC levels at mitotic SPBs and spindle microtubule levels. Quantification of Alp4^{GCP2} (γTuC) and microtubule levels for spindles <3.5 μm in length. The *p* values are from unpaired *t* test: ****$p < 0.0001$, *$p < 0.05$, and ns, $p > 0.05$. (D) The ratio of spindle microtubule to γTuC level increases when Alp16^{GCP6} is expressed. Spindle microtubule level was plotted against Alp4^{GCP2} level using the data used for C. The dotted line was drawn connecting *alp16*Δ and wild-type levels, assuming that the increase in Alp4^{GCP2} level increases spindle microtubule level linearly ($y = 0.69x + 0.31$, where x = Alp4^{GCP2} level and y = spindle microtubule level). Alp16^{GCP6} expression increases spindle microtubule level to higher than the expected value from the equation. The ratio of spindle microtubule to Alp4^{GCP2} level was calculated as a percentage of the expected value and plotted against the Alp4^{GCP2} level. (E) Gfh1^{GCP4} and Mod21^{GCP5} localize to mitotic SPBs when Alp16^{GCP6} is overexpressed in *alp16*Δ cells. Localization of GFP-Gfh1^{GCP4} and GFP- Mod21^{GCP5} was observed in *alp16*Δ cells with P3*nmt*-Alp16 (+T). Scale bar, 10 μm. (F) Gfh1^{GCP4} and Mod21^{GCP5} are not required for Alp16^{GCP6}-dependent γTuC recruitment and spindle microtubule assembly. Alp4^{GCP2} (γTuC) and microtubule levels for spindles <3.5 μm in length were quantified in wild-type, *alp16*Δ, *alp16*Δ with P3-Alp16 (+T), *alp16*Δ *gfh1*Δ with P3-Alp16 (+T), and *alp16*Δ *gfh1*Δ *mod21*Δ cells with P3-Alp16 (+T). The *p* values are from unpaired *t* test: ****$p < 0.0001$, **$p < 0.01$, and ns, $p > 0.05$.

increases the minichromosome loss rate when the spindle assembly checkpoint is inactivated. Thus Alp16^{GCP6}-dependent spindle microtubule assembly ensures faithful chromosome segregation.

GCP6-specific phenotypes of mitotic spindle functions have been observed in other organisms. In *Aspergillus nidulans*, GCPD/GCP4, GCPE/GCP5, and GCPF/GCP6 exhibit a hierarchy of localization to the SPB similar to our results (Xiong and Oakley, 2009). *GCP6*Δ diploid cells lose chromosomes at a higher frequency, and *GCP6*Δ *mad2*Δ diploid cells show more severe synthetic sickness (Xiong and Oakley, 2009). In human cells, down-regulating GCP6 induces a high percentage of monopolar spindles compared with down-regulating GCP4 and GCP5 (Bahtz *et al.*, 2012). These observations suggest that GCP4-6 mitotic functions are substantially conserved in the phylogenetically distant fungi *S. pombe* and *A. nidulans* and partly conserved in fungi and higher eukaryotes.

In contrast to the mitotic phenotypes, a single disruptant of *gfh1*, *mod21*, or *alp16* and double and triple disruptants reduce cytoplasmic microtubule number and interphase MTOC activity to a similar extent (Fujita *et al.*, 2002; Anders *et al.*, 2006), suggesting that the deletion of any γTuRC-specific component disrupts interphase γTuRC function. Differences in the properties of mitotic and interphase γTuRCs may arise from the cell cycle–dependent

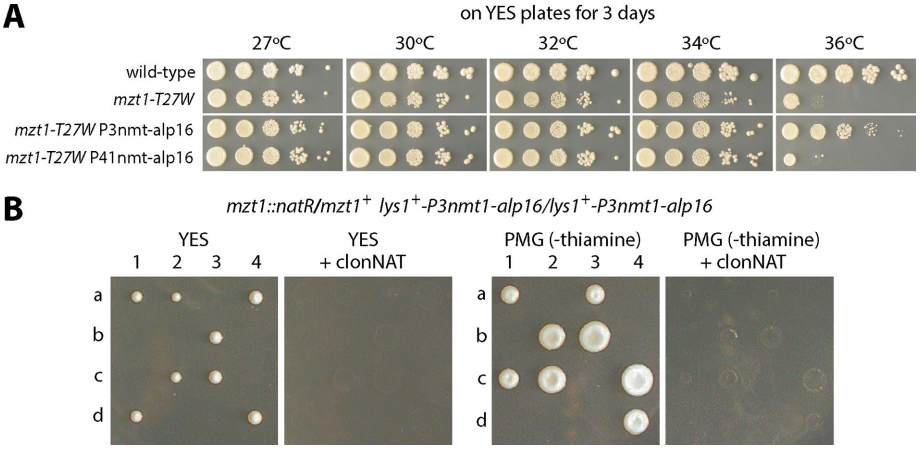

FIGURE 6: Alp16^{GCP6} overproduction suppresses the temperature sensitivity of *mzt1* mutants but not the lethality of *mzt1-null*. (A) The temperature sensitivity of *mzt1-T27W* is rescued by Alp16^{GCP6} overproduction. Serial dilution spot assays of wild-type, *mzt1-T27W*, *mzt1-T27W lys1*$^+$*-P3nmt-alp16*, and *mzt1-T27W lys1*$^+$*-P41nmt-alp16* cells. Cells were spotted onto YES plates and incubated at various temperatures for 3 d. (B) Mzt1 is essential for growth in Alp16^{GCP6}-overproducing cells. Diploid cells homologous for *lys1*$^+$*-P3nmt-alp16* and heterozygous for *mzt1* (*mzt1*$^+$*/mzt1*Δ*::natR*) were sporulated, and individual spores (a–d) in each ascus (1–4) were dissected on YES to partially repress the expression of Alp16^{GCP6} and on PMG plates to highly induce the expression. Only *mzt1*$^+$ segregants sensitive to clonNAT grew in both conditions.

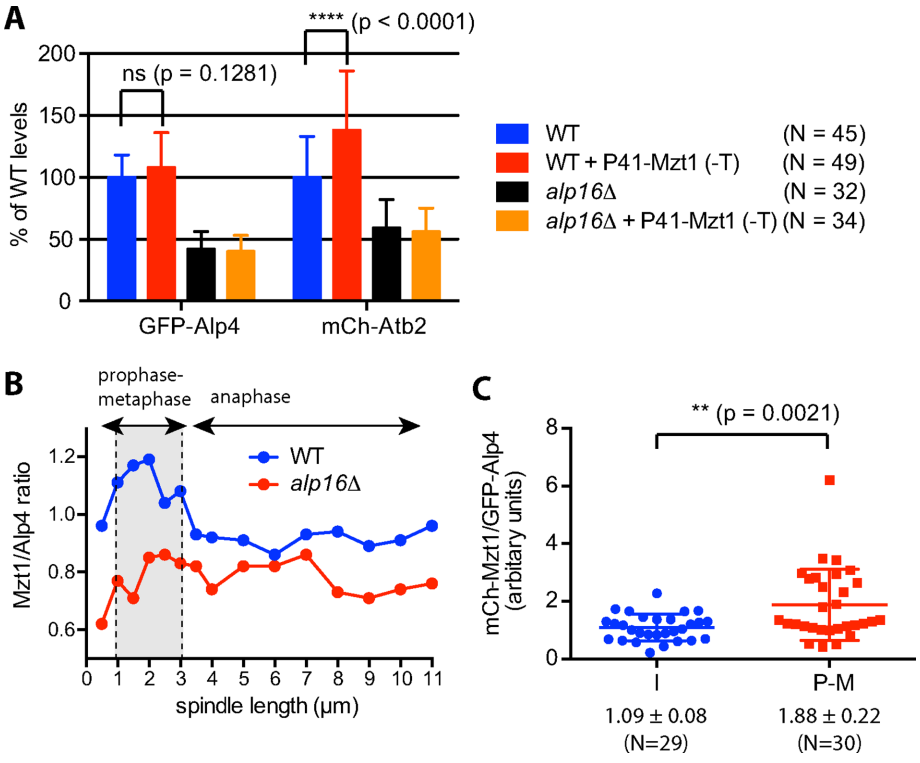

FIGURE 7: Mzt1 plays a role in the activation of the γTuRC ring but not the γTuSC ring. (A) Mzt1 overproduction has no effect on *alp16*Δ cells but increases the spindle microtubule level without increasing the level of γTuC at mitotic SPBs in wild-type cells. Mzt1 was overproduced at the *lys1* locus under the control of P41*nmt* in the absence of thiamine at 27°C for 22 h in wild-type and *alp16*Δ cells containing GFP-Alp4^{GCP2} and mCh-Atb2. Alp4^{GCP2} and Atb2 levels for spindles <3.5 μm in length were quantified. (B) The ratio of Mzt1 to γTuC increases at early M phase in wild-type cells. The ratio of Mzt1 to Alp4^{GCP2} level at mitotic SPBs was calculated in wild-type and *alp16*Δ cells from the data shown in Figure 1, D and E, and plotted against spindle length. (C) The ratio of Mzt1 to γTuC is higher at early M phase than during I phase. The ratio of Mzt1 to Alp4^{GCP2} levels at SPBs for spindles <3.5 μm in length was measured in GFP-Alp4^{GCP2} mCh-Mzt1 cells and compared with that at SPBs during interphase.

modification of the γTuC, which has been suggested by in vitro studies in *S. pombe* (Masuda *et al.*, 1992; Masuda and Shibata, 1996) and shown in vivo in *S. cerevisiae* (Pereira *et al.*, 1998; Vogel *et al.*, 2001; Keck *et al.*, 2011; Lin *et al.*, 2011), or from the mitosis-specific interaction of the γTuC with regulators required for bipolar spindle assembly, such as kinesins (Prigozhina *et al.*, 2001; Rodriguez *et al.*, 2008; Olmsted *et al.*, 2014) and spindle-anchoring factors (Toya *et al.*, 2007; Yukawa *et al.*, 2015). For instance, kinesin-14 binds to the γTuRC and establishes spindle bipolarity (Prigozhina *et al.*, 2001; Olmsted *et al.*, 2014). Alp16-specific mitotic phenotypes may be induced through a mechanism involving this interaction.

Alternatively, it may result from differences in the properties of the mitotic and interphase γTuC receptors. γTuC receptors can be classified by the N-terminal γTuSC-binding motifs (Lin *et al.*, 2014). The mitotic receptor Pcp1 (Flory *et al.*, 2002; Fong *et al.*, 2010) and the interphase receptor Mto1 (Sawin *et al.*, 2004; Lynch *et al.*, 2014) belong to different classes. Pcp1 homologues act as a major receptor in *A. nidulans* and human cells, which exhibit GCP6-specific mitotic phenotypes. The γTuC receptors may define the roles of γTuRC-specific components in spindle assembly.

Assembly of the γTuRC ring

We presume that the γTuRC ring is assembled in the cytoplasm of *S. pombe* cells as shown in other organisms, although there is no direct evidence for its presence. The down-regulation of GCP4, GCP5, or GCP6 disrupts γTuRC in *Drosophila* and human cells. In contrast, it is not clear for *S. pombe* cells whether the deletion of Gfh1^{GCP4}, Mod21^{GCP5}, or Alp16^{GCP6} disrupts the γTuRC ring. Neither gel filtration chromatography (Fujita *et al.*, 2002) nor sucrose gradient centrifugation (Anders *et al.*, 2006; unpublished data) of cell extracts reveals a difference in the distribution pattern of γTuCs between wild-type cells and *alp16*Δ or triple disruptants. These results suggest that γTuRCs assembled during interphase are unstable or too low in number to be detected by conventional methods using asynchronous cell extracts (Anders *et al.*, 2006). The γTuRC may become functional at the onset of mitosis when it interacts with the mitotic receptor at the SPBs. We showed that Alp16^{GCP6} expression in the *gfh1*Δ *mod21*Δ *alp16*Δ triple disruptant is sufficient for maintaining γTuC levels at mitotic SPBs and spindle microtubule levels to an extent similar to wild-type cells (Figure 5). This result raises the

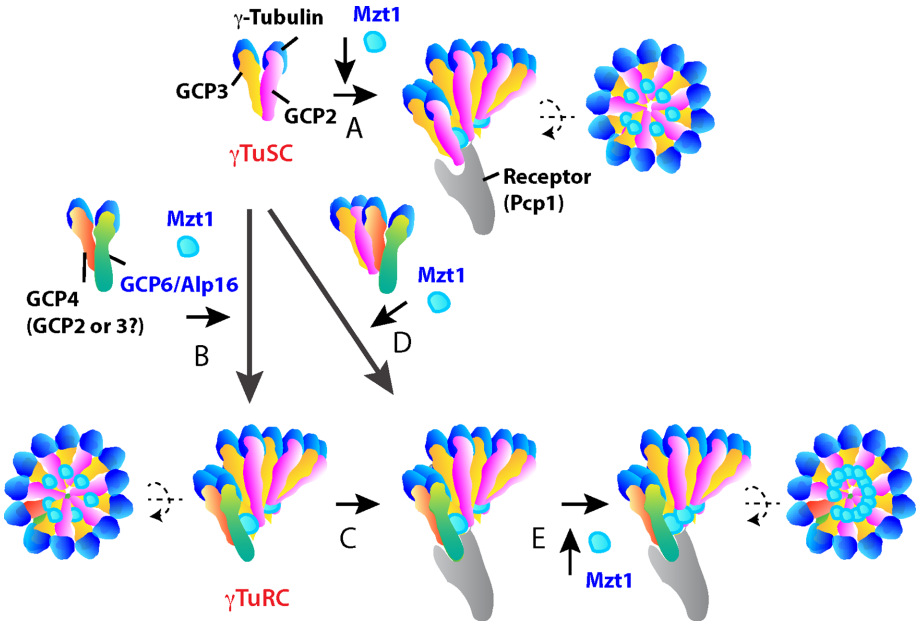

FIGURE 8: Model for the synergistic role of Alp16^{GCP6} and Mzt1 in spindle microtubule assembly. A model for the assembly of γTuSC and γTuRC rings at mitotic SPBs. (A) The γTuSC is recruited to Pcp1, the γTuC receptor at mitotic SPBs, where the γTuSC ring is assembled. Mzt1 is essential for this recruitment. (B) The γTuRC ring is assembled in the presence of Alp16^{GCP6}. Alp16^{GCP6} binds to Gfh1^{GCP4} and to Alp4^{GCP2} or Alp6^{GCP3} in the absence of Gfh1^{GCP4}. (C) The γTuRC ring is recruited to Pcp1 at mitotic SPBs in the presence of Mzt1. This recruitment occurs more efficiently than with γTuSC ring assembly at mitotic SPBs. (D) Alp16^{GCP6} promotes γTuRC ring assembly at mitotic SPBs in the presence of Mzt1. (E) Mzt1 fully activates the γTuRC at mitotic SPBs.

possibility that the γTuRC is assembled in the cytoplasm without Gfh1^{GCP4} and Mod21^{GCP5} at early M phase (Figure 8B). In the absence of Gfh1^{GCP4} and Mod21^{GCP5}, Alp16^{GCP6} may use Alp4^{GCP2} or Alp3^{GCP3} to initiate assembly of the γTuRC (Figure 8B).

Alternatively, only partial γTuC rings of various sizes may be assembled in the cytoplasm of *S. pombe* both in the presence and absence of Alp16^{GCP6}. The complete γTuRC ring may be assembled at mitotic SPBs in the presence of Alp16^{GCP6} and Mzt1 (Figure 8D). Studies of the *S. cerevisiae* γTuSC suggest that it is assembled at the SPB but not in the cytoplasm (Kollman *et al.*, 2010; Erlemann *et al.*, 2012; Lin *et al.*, 2014). In *alp16*Δ *mod21*Δ *gfh1*Δ cells, only γTuSCs are present, and therefore the γTuSC ring presumably is assembled at the MTOCs from γTuSC or partial γTuSC rings (Figure 8A). Expression of Alp16^{GCP6} in the triple disruptant would induce Alp16^{GCP6} binding to the γTuSC (Anders *et al.*, 2006). The Alp16^{GCP6}-γTuSC complex may promote γTuRC ring assembly more efficiently at mitotic SPBs when bound to Pcp1 in the presence of Mzt1 (Figure 8D). In vitro reconstitution of the γTuRC ring in the presence of Pcp1 may clarify the role of Alp16^{GCP6} in ring formation.

Synergistic role of Alp16^{GCP6} and Mzt1 in spindle microtubule assembly

Although Alp16^{GCP6} promotes recruitment of the γTuRC to mitotic SPBs and suppresses the temperature sensitivity of the *mzt1* mutant, Alp16^{GCP6} does not act alone as a recruitment factor but in conjugation with Mzt1 (Figure 6). The increase in Alp16^{GCP6} expression levels results in an increase in γTuC levels at mitotic SPBs, which may be due to either Mzt1-dependent attachment of the preformed γTuRC to mitotic SPBs (Figure 8, B and C), Mzt1-dependent assembly of γTuRC at mitotic SPBs (Figure 8D), or both. These processes may be more efficient than the γTuSC ring assembly at SPBs (Figure 8A). In contrast, elevated Mzt1 expression in *alp16*Δ and wild-type cells does not affect levels of γTuC at SPBs, suggesting that Mzt1 does not act as a rate-limiting factor for γTuC ring formation at SPBs.

We found that Mzt1 overproduction enhances spindle microtubule assembly at mitotic SPBs in wild-type but not in *alp16*Δ cells. The ratio of Mzt1 to Alp4^{GCP2} increases at early M phase in wild-type cells, suggesting that Mzt1 has an additional role in the activation of the γTuRC for spindle microtubule assembly at early M phase (Figure 8E). MOZART1 has been shown to bind GCP3 in *Arabidopsis* and *S. pombe* cells (Janski *et al.*, 2008, 2012; Nakamura *et al.*, 2012; Dhani *et al.*, 2013). Mzt1 forms oligomers in vitro, supporting a model in which the Mzt1 oligomer stabilizes the γTuC ring to produce more efficient microtubule nucleation (Dhani *et al.*, 2013). In *Arabidopsis*, MOZART1/GIP1a-containing γTuC seems to represent a subset of γTuCs that is more competent for microtubule nucleation (Nakamura *et al.*, 2012), suggesting a role for MOZART1 in γTuRC activation. We propose that Mzt1, presumably in an oligomerized state, fully activates mitotic γTuRCs for microtubule nucleation. Alp16^{GCP6} and Mzt1 are crucial for spatiotemporal regulation of microtubule nucleation from the γTuRC and function synergistically at early M phase for efficient bipolar spindle assembly.

MATERIALS AND METHODS

Yeast methods and strains

The *S. pombe* strains used in this study are listed in Supplemental Table S1. Fission yeast media, growth conditions, and manipulations were carried out as previously described (Moreno *et al.*, 1991). For the minichromosome loss assay, strains carrying a minichromosome Ch16 (Niwa *et al.*, 1986) were constructed with the *ade6-M210* background. Because Ch16 had the *ade6-M216* mutation, strains constructed showed the *ade*$^+$ phenotype due to intragenic complementation, and the loss of Ch16 resulted in the *ade*$^-$ phenotype detected by red colony or red-sectored colony formation on plates containing low concentrations of adenine. Strains carrying Ch16 were grown in yeast extract and supplements (YES) medium overnight, spread on YE agar plates at ~200 cells/plate, and grown at 27°C for 6 d. The ratio (percentage) of the number of red-sectored colonies to the number of white- and red-sectored colonies combined was calculated as the minichromosome loss rate. For the overproduction of Alp16^{GCP6}, Alp16^{GCP6} was expressed under thiamine-repressive promoters at the *lys1* locus in *alp16*Δ cells. The *alp16*$^+$ gene was subcloned into pCSU64, 71, and 72 (Chikashige *et al.*, 2004) after GFP was removed from the vectors. pCSU64, 71, and 72 had thiamine-repressive promoters P3*nmt*, P41*nmt*, and P81*nmt*, respectively, for gene expression. The resulting constructs were used for integration of the gene at the *lys1* locus. Cells constructed were incubated at 27°C for 22–24 h in Edinburgh minimal medium 2 (EMM2) supplemented with all growth requirements (amino acids, purines, and pyrimidines) in the presence and absence of 2 μM thiamine. For the construction of strains carrying proteins

with N-terminal GFP, mCh, and GBP, the promoter region of the gene of interest was PCR amplified and inserted at the *Bam*HI site between a selection marker *kanR* and GFP of pCSS25, mCh of pCSS25-mCh (Masuda *et al.*, 2013), and GBP of pCSS25-GBP. pCSS25-GBP was constructed by replacing the GFP of pCSS25 with GBP. The resulting plasmids were used as templates for PCR-based gene targeting. To examine whether Alp16^{GCP6} overproduction rescued the lethality of *mzt1*-null cells, a diploid strain (HR3206) was constructed that was homologous for *lys1*$^{+}$*-P3nmt-alp16* and heterozygous for *mzt1* (*mzt1*$^{+}$*/mzt1*Δ*::natR*). The diploid cells were sporulated and dissected on YES agar plates to partially suppress the expression of Alp16^{GCP6} and on EMM2 and PMG agar plates to fully induce the expression. Pombe medium glutamate (PMG) was the same as EMM2 except that it contained 3.75 g/l L-glutamic acid monosodium salt instead of NH_4Cl. The resistance of viable spores for clonNAT was checked on YES or PMG plates at 100 μg/ml.

Fluorescence microscopy

Fluorescence microscope images were obtained using the DeltaVision microscope system (Applied Precision, Seattle, WA) with a CoolSNAP.HQ cooled charge-coupled device camera (Photometrics, Tucson, AZ) equipped with a temperature-controlled chamber (Precision Control, Seattle, WA). Live cells were imaged in a glass-bottom culture dish (MatTek, Ashland, MA) coated with soybean lectin at 27°C. For quantification of fluorescent protein levels, images of 12–14 sections were taken along the *z*-axis at 0.3-μm intervals. After deconvolution, projection images of maximum intensity were obtained, and maximum fluorescence intensities over the background intensity were used for statistical data analysis. In some experiments, sum intensity images were obtained from five image stacks (a 0.3-μm stack distance) with the stack containing the highest signal intensity in the middle. A 5 × 5–pixel (0.5375-μm square) region of interest (ROI) with maximum sum intensity was determined for each mitotic SPB. Sum intensity of two 20 × 20–pixel regions around the ROI was used for background subtraction. The data from projection images of maximum intensity were used for all of the analysis, since similar ratios of fluorescence intensity in *alp16*Δ to wild-type cells were obtained using quantification from projection images of the maximum intensity and the sum intensity (Supplemental Figure S2A). Time-lapse imaging was performed by taking images every 1 min for 30 min or every 2 min for 40 min. Spindles formed at 2–10 min after start of observation were selected for analysis. To avoid any effect of photobleaching, cells were observed only under bright field before the fluorescence images were taken. All of the data, except for time-lapse imaging shown in Figures 2 and 3, were obtained from still images (a single time point with *z*-sectioning).

To test whether an internal fluorescence control is necessary for comparison of GFP levels in wild-type and *alp16*Δ cells, Sid4-mRFP signal intensities at SPBs were measured as internal controls, and GFP intensities relative to mRFP intensities at SPBs (GFP/mRFP ratios) were compared between wild-type and *alp16*Δ cells. The data obtained from the GFP/mRFP ratios were virtually identical to those obtained from GFP intensity in wild-type and *alp16*Δ cells (Supplemental Figure S2, C–I).

ACKNOWLEDGMENTS

We thank Frank Uhlmann and Julie Cooper for allowing work for revision of the manuscript to be carried out in their laboratories. We thank Ken Sawin, Yuji Chikashige, and Yasushi Hiraoka for reagents and Risa Mori for critical reading of the manuscript. This work was supported by Cancer Research UK, the Francis Crick Institute, Hiroshima University, and the Japan Society for the Promotion of Science KAKENHI Scientific Research (A) (16H02503) and Challenging Exploratory Research (16K14672) (T.T.).

REFERENCES

Anders A, Lourenco PC, Sawin KE (2006). Noncore components of the fission yeast γ-tubulin complex. Mol Biol Cell 17, 5075–5093.

Bahtz R, Seidler J, Arnold M, Haselmann-Weiss U, Antony C, Lehmann WD, Hoffmann I (2012). GCP6 is a substrate of Plk4 and required for centriole duplication. J Cell Sci 125, 486–496.

Basi G, Schmid E, Maundrell K (1993). TATA box mutations in the *Schizosaccharomyces pombe nmt*1 promoter affect transcription efficiency but not the transcription start point or thiamine repressibility. Gene 123, 131–136.

Chikashige Y, Kurokawa R, Haraguchi T, Hiraoka Y (2004). Meiosis induced by inactivation of Pat1 kinase proceeds with aberrant nuclear positioning of centromeres in the fission yeast *Schizosaccharomyces pombe*. Genes Cells 9, 671–684.

Dhani DK1, Goult BT, George GM, Rogerson DT, Bitton DA, Miller CJ, Schwabe JW, Tanaka K (2013). Mzt1/Tam4, a fission yeast MOZART1 homologue, is an essential component of the γ-tubulin complex and directly interacts with GCP3^{Alp6}. Mol Biol Cell 24, 3337–3349.

Erlemann S, Neuner A, Gombos L, Gibeaux R, Antony C, Schiebel E (2012). An extended γ-tubulin ring functions as a stable platform in microtubule nucleation. J Cell Biol 197, 59–74.

Flory MR, Morphew M, Joseph JD, Means AR, Davis TN (2002). Pcp1p, an Spc110p-related calmodulin target at the centrosome of the fission yeast *Schizosaccharomyces pombe*. Cell Growth Differ 13, 47–58.

Fong CS, Sato M, Toda T (2010). Fission yeast Pcp1 links polo kinase-mediated mitotic entry to γ-tubulin-dependent spindle formation. EMBO J 29, 120–130.

Fujita A, Vardy L, Garcia MA, Toda T (2002). A fourth component of the fission yeast γ-tubulin complex, Alp16, is required for cytoplasmic microtubule integrity and becomes indispensable when γ-tubulin function is compromised. Mol Biol Cell 13, 2360–2373.

Guillet V, Knibiehler M, Gregory-Pauron L, Remy MH, Chemin C, Raynaud-Messina B, Bon C, Kollman JM, Agard DA, Merdes A, Mourey L (2011). Crystal structure of γ-tubulin complex protein GCP4 provides insight into microtubule nucleation. Nat Struct Mol Biol 18, 915–919.

Gunawardane RN, Martin OC, Zheng Y (2003). Characterization of a new γTuRC subunit with WD repeats. Mol Biol Cell 14, 1017–1026.

Hutchins JR, Toyoda Y, Hegemann B, Poser I, Hériché JK, Sykora MM, Augsburg M, Hudecz O, Buschhorn BA, Bulkescher J, *et al*. (2010). Systematic analysis of human protein complexes identifies chromosome segregation proteins. Science 328, 593–599.

Izumi N, Fumoto K, Izumi S, Kikuchi A (2008). GSK-3β regulates proper mitotic spindle formation in cooperation with a component of the γ-tubulin ring complex, GCP5. J Biol Chem 283, 606–613.

Janski N, Herzog E, Schmit AC (2008). Identification of a novel small *Arabidopsis* protein interacting with γ-tubulin complex protein 3. Cell Biol Int 32, 546–548.

Janski N, Masoud K, Batzenschlager M, Herzog E, Evrard JL, Houlne G, Bourge M, Chaboute ME, Schmit AC (2012). The GCP3-interacting proteins GIP1 and GIP2 are required for γ-tubulin complex protein localization, spindle integrity, and chromosomal stability. Plant Cell 24, 1171–1187.

Keck JM, Jones MH, Wong CC, Binkley J, Chen D, Jaspersen SL, Holinger EP, Xu T, Niepel M, Rout MP, *et al.* (2011). A cell cycle phosphoproteome of the yeast centrosome. Science 332, 1557–1561.

Kollman JM, Merdes A, Mourey L, Agard DA (2011). Microtubule nucleation by γ-tubulin complexes. Nat Rev Mol Cell Biol 12, 709–721.

Kollman JM, Polka JK, Zelter A, Davis TN, Agard DA (2010). Microtubule nucleating γ-TuSC assembles structures with 13-fold microtubule-like symmetry. Nature 466, 879–882.

Lin TC, Gombos L, Neuner A, Sebastian D, Olsen JV, Hrle A, Benda C, Schiebel E (2011). Phosphorylation of the yeast γ-tubulin Tub4 regulates microtubule function. PLoS One 6, e19700.

Lin TC, Neuner A, Schiebel E (2015). Targeting of γ-tubulin complexes to microtubule organizing centers: conservation and divergence. Trends Cell Biol 25, 296–307.

Lin TC, Neuner A, Schlosser YT, Scharf AN, Weber L, Schiebel E (2014). Cell-cycle dependent phosphorylation of yeast pericentrin regulates γ-TuSC-mediated microtubule nucleation. Elife 3, e02208.

Lynch EM, Groocock LM, Borek WE, Sawin KE (2014). Activation of the γ-tubulin complex by the Mto1/2 complex. Curr Biol 24, 896–903.
Masuda H, Mori R, Yukawa M, Toda T (2013). Fission yeast MOZART1/Mzt1 is an essential γ-tubulin complex component required for complex recruitment to the microtubule organizing center, but not its assembly. Mol Biol Cell 24, 2894–2906.
Masuda H, Sevik M, Cande WZ (1992). In vitro microtubule-nucleating activity of spindle pole bodies in fission yeast *Schizosaccharomyces pombe*: cell cycle-dependent activation in *Xenopus* cell-free extracts. J Cell Biol 117, 1055–1066.
Masuda H, Shibata T (1996). Role of γ-tubulin in mitosis-specific microtubule nucleation from the *Schizosaccharomyces pombe* spindle pole body. J Cell Sci 109, 165–177.
Moreno S, Klar A, Nurse P (1991). Molecular genetic analyses of fission yeast *Schizosaccharomyces pombe*. Methods Enzymol 194, 773–782.
Moritz M, Braufeld MB, Dedat JW, Alberts B, Agard DA (1995). Microtubule nucleation by γ-tubulin-containing rings in the centrosome. Nature 378, 638–640.
Moritz M, Braunfeld MB, Guenebaut V, Heuser J, Agard DA (2000). Structure of the γ-tubulin ring complex: a template for microtubule nucleation. Nat Cell Biol 2, 365–370.
Murphy SM, Preble AM, Patel UK, O'Connell KL, Dias DP, Moritz M, Agard D, Stults JT, Stearns T (2001). GCP5 and GCP6: two new members of the human γ-tubulin complex. Mol Biol Cell 12, 3340–3352.
Nakamura M, Yagi N, Kato T, Fujita S, Kawashima N, Ehrhardt DW, Hashimoto T (2012). *Arabidopsis* GCP3-interacting protein 1/MOZART1 is an integral component of the γ-tubulin-containing microtubule nucleating complex. Plant J 71, 216–225.
Niwa O, Matsumoto T, Yanagida M (1986). Construction of a mini-chromosome by deletion and its mitotic and meiotic behavior in fission yeast. Mol Gen Genet 203, 397–405.
Oakley BR, Paolillo V, Zheng Y (2015). γ-Tubulin complexes in microtubule nucleation and beyond. Mol Biol Cell 26, 2957–2962.
Oegema K, Wiese C, Martin OC, Milligan RA, Iwamatsu A, Mitchison TJ, Zheng Y (1999). Characterization of two related *Drosophila* γ-tubulin complexes that differ in their ability to nucleate microtubules. J Cell Biol 144, 721–733.
Olmsted ZT, Colliver AG, Riehlman TD, Paluh JL (2014). Kinesin-14 and kinesin-5 antagonistically regulate microtubule nucleation by γ-TuRC in yeast and human cells. Nat Commun 5, 5339.
Pereira G, Knop M, Schiebel E (1998). Spc98p directs the yeast γ-tubulin complex into the nucleus and is subject to cell cycle-dependent phosphorylation on the nuclear side of the spindle pole body. Mol Biol Cell 9, 775–793.
Petry S, Vale RD (2015). Microtubule nucleation at the centrosome and beyond. Nat Cell Biol 17, 1089–1093.
Prigozhina NL, Walker RA, Oakley CE, Oakley BR (2001). γ-Tubulin and the C-terminal motor domain kinesin-like protein, KLPA, function in the establishment of spindle bipolarity in Aspergillus nidulans. Mol Biol Cell 12, 3161–3174.
Rodriguez AS, Batac J, Killilea AN, Filopei J, Simeonov DR, Lin I, Paluh JL (2008). Protein complexes at the microtubule organizing center regulate bipolar spindle assembly. Cell Cycle 7, 1246–1253.
Rothbauer U, Zolghadr K, Muyldermans S, Schepers A, Cardoso MC, Leonhardt H (2008). A versatile nanotrap for biochemical and functional studies with fluorescent fusion proteins. Mol Cell Proteomics 7, 282–289.
Sawin KE, Lourenco PC, Snaith HA (2004). Microtubule nucleation at non-spindle pole body microtubule-organizing centers requires fission yeast centrosomin-related protein mod20p. Curr Biol 14, 763–775.
Schnorrer F, Luschnig S, Koch I, Ngüslein-Volhard C (2002). Gamma-tubulin37C and gamma-tubulin ring complex protein 75 are essential for bicoid RNA localization during *Drosophila* oogenesis. Dev Cell 3, 685–696.
Teixidó-Travesa N, Roig J, Lüders J (2012). The where, when and how of microtubule nucleation—one ring to rule them all. J Cell Sci 125, 4445–4456.
Teixidó-Travesa N, Villen J, Lacasa C, Bertran MT, Archinti M, Gygi SP, Caelles C, Roig J, Lüders J (2010). The γTuRC revisited: a comparative analysis of interphase and mitotic human γTuRC redefines the set of core components and identifies the novel subunit GCP8. Mol Biol Cell 21, 3963–3972.
Toya M, Sato M, Haselmann U, Asakawa K, Brunner D, Antony C, Toda T (2007). γ-Tubulin complex-mediated anchoring of spindle microtubules to spindle-pole bodies requires Msd1 in fission yeast. Nat Cell Biol 9, 646–653.
Vardy L, Toda T (2000). The fission yeast γ-tubulin complex is required in G1 phase and is a component of the spindle assembly checkpoint. EMBO J 19, 6098–6111.
Venkatram S, Tasto JJ, Feoktistova A, Jennings JL, Link AJ, Gould KL (2004). Identification and characterization of two novel proteins affecting fission yeast γ-tubulin complex function. Mol Biol Cell 15, 2287–2301.
Verollet C, Colombie N, Daubon T, Bourbon HM, Wright M, Raynaud-Messina B (2006). *Drosophila melanogaster* γ-TuRC is dispensable for targeting γ-tubulin to the centrosome and microtubule nucleation. J Cell Biol 172, 517–528.
Vogel J, Drapkin B, Oomen J, Beach D, Bloom K, Snyder M (2001). Phosphorylation of γ-tubulin regulates microtubule organization in budding yeast. Dev Cell 1, 621–631.
Xiong Y, Oakley BR (2009). In vivo analysis of the functions of γ-tubulin-complex proteins. J Cell Sci 122, 4218–4227.
Yukawa M, Ikebe C, Toda T (2015). The Msd1-Wdr8-Pkl1 complex anchors microtubule minus ends to fission yeast spindle pole bodies. J Cell Biol 209, 549–562.
Zhang L, Keating TJ, Wilde A, Borisy GG, Zheng Y (2000). The role of Xgrip210 in γ-tubulin ring complex assembly and centrosome recruitment. J Cell Biol 151, 1525–1536.
Zheng Y, Wong ML, Alberts B, Mitchison T (1995). Nucleation of microtubule assembly by a γ-tubulin-containing ring complex. Nature 378, 578–583.